Crystal and Molecular Structure of Antibiotic Gilvocarcin M

Noriaki HIRAYAMA,* Keiichi TAKAHASHI, Kunikatsu SHIRAHATA,
Yuji OHASHI,† and Yoshio SASADA†

Tokyo Research Laboratory, Kyowa Hakko Kogyo Co., Ltd., 3-6-6 Asahimachi, Machida, Tokyo 194

†*Laboratory of Chemistry for Natural Products, Tokyo Institute of Technology, Nagatsuta, Midori-ku, Yokohama 227*

(Received November 8, 1980)

The structure of gilvocarcin M, $C_{26}H_{26}O_9$, an antibiotic with a novel carbon skeleton, has been determined by single crystal X-ray analysis. The space group is $P2_1$ with $a=15.063(5)$, $b=16.162(4)$, $c=4.905(2)$ Å, $\beta=91.47(3)°$, and $Z=2$. The structure was solved by direct methods, and least-squares refinement using 1734 reflexions gave the final R value of 0.054. The title compound is composed of a unique aglycone and a fucofuranose, which are linked together through a C–C glycosyl linkage. The furanose ring takes the $^{\circ}E$ conformation.

Gilvocarcin M and V are antibiotics produced by *Streptomyces gilvotanareus* and *Streptomyces griseologilbus*.[1] They were called previously DC-38.[2] Their structures have been elucidated on the basis of their chemical nature and spectroscopic data.[3] The structural difference between M and V is that a methyl group at C(22) in the former is replaced by a vinyl group in the latter. The structure of gilvocarcin M and the numbering system is shown in Fig. 1. In spite of many efforts with various kinds of NMR techniques including proton-proton spin decoupling and ^{13}C-NMR with long range selective proton decoupling, there has still remained some ambiguity especially around the asymmetric carbons of the furanose. To determine the structure of gilvocarcins unequivocally, we have undertaken an X-ray analysis of gilvocarcin M. This paper will describe the crystal structure of the antibiotic.

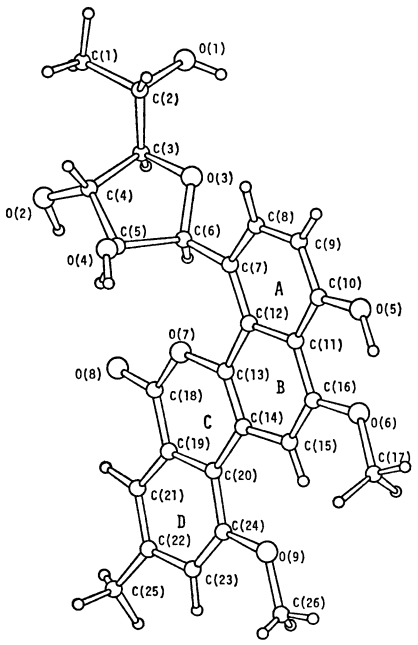

Fig. 1. The numbering system of gilvocarcin M.

Experimental and Structure Determination

Yellow prismatic crystals of gilvocarcin M were obtained from a DMSO–ethanol solution. A crystal, $0.5\times0.13\times0.05$ mm^3, was used for data collection on a Rigaku four-circle automated diffractometer with Ni-filtered Cu $K\alpha$ radiation. Preliminary unit cell dimensions and space group were obtained from oscillation and Weissenberg photographs. The space group was determined from systematic absences ($0k0$ for odd k). Accurate cell dimensions were determined by a least-squares calculation with 2θ values of 16 high-angle reflexions measured on the diffractometer. Crystal data are summarized in Table 1. All independent reflexions within the range $2\theta\leqq120°$ were collected by use of the ω-2θ scan mode with a scanning rate of $4°(2\theta)\text{min}^{-1}$. Stationary background counts were accumulated for 10 s before and after each scan. Periodic checks of the intensity values of three standard reflexions showed no significant X-ray damage. Corrections for absorption or extinction were not applied. Out of 1847 independent reflexions obtained, 1735 for which $|F_o|>3.0\sigma(|F_o|)$ were used.

TABLE 1.

$C_{26}H_{26}O_9\cdot0.4C_2H_6O$	$b=16.162(4)$ Å
$M.W.=500.9$	$c=4.905(2)$ Å
$P2_1$	$\beta=91.47(3)°$
$Z=2$	$D_x=1.393$ g cm^{-3}
$a=15.063(5)$Å	μ(Cu $K\alpha$) $=21.47$ cm^{-1}

The phases of 339 reflexions with $|E_o|\geqq1.2$ were assigned with MULTAN.[4] The best set of phases was used to calculate an E-map, which gave 21 chemically significant peaks. Other 15 non-hydrogen atoms were found by the successive Fourier syntheses. The structural parameters were refined by block-diagonal least-squares with a modified HBLS programme. All the hydrogen atoms and a molecule of the ethanol solvent without hydrogen atoms were found by the difference syntheses. Refinement gave the final R value 0.054 for 1734 reflexions. The atoms of the solvent molecules with the occupancy of 0.4 were refined isotropically. The weighting system used in the final stage was $w=0.3$ for $|F_o|<1.782$ and $|F_o|>17.82$, and $w=(0.00115(F_o)^2-0.12675|F_o|+4.48559)^{-1}$ for $1.782\leqq|F_o|\leqq17.82$. A strong reflexion, 020, was excluded because it seemed to suffer from secondary extinction. Atomic scattering factors were taken from "International Tables for X-Ray Crystallography."[5] The final positional and thermal parameters are given in Table 2. The tables of anisotropic temperature factors and observed and calculated structure factors are kept as a Document No. 8132 at the Chemical Society of Japan.

Results and Discussion

Molecular Structure. Bond lengths and angles are tabulated in Table 3. A stereoscopic drawing of the molecule is shown in Fig. 2. The two bonds C(15)–C(16) and C(18)–O(7), which correspond to K region of phenantherene,[6] show rather high double bond character. There is an intramolecular hydrogen bond between O(5) and O(6) atoms; O(5)···O(6)= 2.547(6) Å, H(O(5))···O(6)=1.68(7) Å, and O(5)–H···O(6) angle is 141.2°. Although the reason is not clear, the C(24)–O(9) length is significantly shorter than the C(16)–O(16).

The C–C glycosyl bond length, C(6)–C(7), is somewhat longer than the corresponding values (1.492—1.501 Å) in formycin.[7] In usual nucleosides C(4')–O(1') is significantly longer than C(1')–O1(1'). In gilvocarcin M, however, C(6)–O(3) is significantly longer than C(3)–O(3). There are two short intramolecular non-bonded contacts; O(3)···C(8)=2.622(7) Å and O(7)···C(6)=2.682(6) Å.

The least-squares planes of interest and the dihedral angles between them are tabulated in Table 4. The aglycone part except the substituents is planar within ±0.1 Å. Although every six-membered rings are planar, the planarity of the D ring is best (±0.008 Å) and that of the C ring is worst (±0.035 Å). The dihedral angles between the rings A and B, between rings B and C, and between rings C and D are 1.9, 2.3, and 2.4°, respectively. These values show a smooth convex character of the aglycone part, as seen in Fig. 3, the side view of the molecule. The dihedral angles between the least-squares planes of furanose ring and the aglycone part is 53.5°.

The O(3) atom deviates by 0.531 Å from the plane determined by the C(3), C(4), C(5), and C(6) atoms, and the puckering parameters P and θ_m[8] are 94.8 and 39.9°, respectively. This indicates that the furanose ring takes an unusual $^{\circ}E$ conformation. It is probable that the $^{\circ}E$ conformation is related to the above-mentioned bond length reversion at the C(3)–O(3) and C(6)–O(3) bonds. The conformation around the C(2)–C(3) bond is *gauche-trans*, and the χ_{cc} angle of 19.7° is in the *anti* region. Torsional angles are listed in Table 5.

Crystal Structure. A stereoscopic drawing of the crystal structure viewed along the c axis is shown in Fig. 4. There are three intermolecular OH···O hydrogen bonds as listed in Table 6. Between the

Table 2. Fractional atomic coordinates with their standard deviations and temperature factors

Atom	x	y	z	B_{eq} or B/Å^2	Atom	x	y	z	B_{eq} or B/Å^2
C(1)	−0.0849(4)	0.2055(5)	0.0166(19)	6.40	O(7)	0.3602(2)	0.3430(2)	0.0540(7)	2.81
C(2)	−0.0406(4)	0.2852(5)	0.1113(14)	4.97	O(8)	0.3800(2)	0.2557(2)	−0.2808(7)	3.31
C(3)	0.0574(3)	0.2879(4)	0.0555(12)	3.63	O(9)	0.6652(3)	0.4619(3)	0.2373(9)	4.89
C(4)	0.1124(4)	0.2152(3)	0.1634(11)	3.47	HAC(1)	−0.165(5)	0.215(5)	−0.163(17)	7.6
C(5)	0.2000(3)	0.2542(3)	0.2703(10)	3.00	HBC(1)	−0.077(5)	0.192(5)	−0.163(17)	9.4
C(6)	0.1897(3)	0.3471(3)	0.1973(10)	2.96	HCC(1)	−0.061(5)	0.151(5)	0.114(16)	8.0
C(7)	0.2292(3)	0.4112(3)	0.3907(10)	2.92	HC(2)	−0.057(4)	0.297(5)	0.303(12)	6.3
C(8)	0.1720(4)	0.4471(4)	0.5688(11)	3.55	HC(3)	0.072(3)	0.295(3)	−0.127(9)	2.8
C(9)	0.1985(4)	0.5083(4)	0.7573(12)	3.75	HC(4)	0.080(3)	0.187(3)	0.330(11)	3.9
C(10)	0·2830(4)	0.5353(3)	0.7661(10)	3.35	HC(5)	0.254(3)	0.232(3)	0.171(8)	1.7
C(11)	0.3473(3)	0.5021(3)	0.5896(10)	2.93	HC(6)	0.216(4)	0.354(4)	0.016(11)	4.7
C(12)	0.3192(3)	0.4377(3)	0.3988(10)	2.66	HC(8)	0.114(3)	0.435(3)	0.592(9)	2.3
C(13)	0.3890(3)	0.4053(3)	0.2321(10)	2.88	HC(9)	0.158(3)	0.531(3)	0.887(11)	3.5
C(14)	0.4758(3)	0.4291(3)	0.2402(9)	2.63	HC(15)	0.557(3)	0.515(3)	0.412(9)	2.9
C(15)	0.4989(4)	0.4946(4)	0.4242(10)	3.34	HAC(17)	0.578(4)	0.643(4)	0.634(12)	5.5
C(16)	0.4369(4)	0.5278(3)	0.5845(10)	3.15	HBC(17)	0.552(9)	0.658(9)	1.008(28)	11.7
C(17)	0.5517(4)	0.6122(4)	0.8013(14)	4.82	HCC(17)	0.597(5)	0.562(1)	0.838(15)	7.6
C(18)	0.4140(3)	0.3061(3)	−0.1233(10)	2.67	HC(21)	0.531(4)	0.240(4)	−0.391(12)	6.0
C(19)	0.5081(3)	0.3254(3)	−0.1118(10)	2.84	HC(23)	0.750(3)	0.362(3)	−0.091(3)	3.7
C(20)	0.5397(3)	0.3874(3)	0.0683(10)	2.98	HAC(25)	0.768(4)	0.280(5)	−0.473(13)	7.0
C(21)	0.5640(3)	0.2817(4)	−0.2811(10)	3.26	HBC(25)	0.701(5)	0.240(6)	0.365(16)	9.3
C(22)	0.6537(4)	0.2965(4)	−0.2789(11)	3.53	HCC(25)	0.739(5)	0.202(4)	−0.368(14)	7.1
C(23)	0.6872(3)	0.3582(4)	−0.1044(12)	3.76	HAC(26)	0.775(5)	0.498(5)	−0.005(15)	8.8
C(24)	0.6324(3)	0.4025(4)	0.0649(12)	3.45	HBC(26)	0.759(4)	0.464(4)	0.273(11)	4.6
C(25)	0.7152(4)	0.2476(5)	−0.4535(12)	8.03	HCC(26)	0.764(5)	0.528(5)	0.353(15)	8.0
C(26)	0.7590(5)	0.4812(6)	0.2429(20)	8.03	HO(1)	−0.062(5)	0.404(5)	0.009(15)	7.8
O(1)	−0.0856(3)	0.3500(4)	−0.0246(16)	8.92	HO(2)	0.170(5)	0.168(5)	−0.165(16)	9.2
O(2)	0.1247(3)	0.1515(3)	−0.0341(8)	4.16	HO(4)	0.264(4)	0.240(5)	0.590(13)	6.1
O(3)	0.0943(2)	0.3590(2)	0.1823(8)	3.43	HO(5)	0.368(4)	0.613(4)	0.939(13)	6.0
O(4)	0.2064(2)	0.2401(3)	0.5590(7)	3.54	O_{et}	0.0302(8)	0.0132(8)	−0.2667(25)	5.5
O(5)	0.3038(3)	0.5948(3)	0.9560(8)	4.29	$C(1)_{et}$	0.0250(11)	0.0083(12)	0.0333(38)	6.0
O(6)	0.4600(3)	0.5913(3)	0.7694(8)	4.44	$C(2)_{et}$	0.0469(14)	0.0021(13)	0.1974(38)	10.1

TABLE 3. BOND LENGTHS (l/Å) AND ANGLES (ϕ/°)

C(1)-C(2)	1.517(12)	C(2)-O(1)	1.406(11)	C(2)-C(3)	1.509(10)
C(3)-C(4)	1.524(8)	C(4)-C(5)	1.543(8)	C(4)-O(2)	1.429(7)
C(5)-C(6)	1.549(8)	C(5)-O(4)	1.435(7)	C(6)-O(3)	1.449(7)
C(3)-O(3)	1.415(7)	C(6)-C(7)	1.517(7)	C(7)-C(8)	1.371(8)
C(8)-C(9)	1.405(8)	C(9)-C(10)	1.346(8)	C(10)-C(11)	1.421(8)
C(11)-C(12)	1.455(7)	C(12)-C(7)	1.421(7)	C(10)-O(5)	1.369(7)
C(16)-O(6)	1.407(7)	O(6)-C(17)	1.426(8)	C(12)-C(13)	1.447(7)
C(13)-C(14)	1.363(7)	C(14)-C(15)	1.428(8)	C(15)-C(16)	1.348(8)
C(16)-C(11)	1.413(7)	C(13)-O(7)	1.394(6)	C(14)-C(20)	1.461(7)
C(18)-O(7)	1.343(6)	C(18)-O(8)	1.225(6)	C(18)-C(19)	1.451(7)
C(19)-C(20)	1.410(7)	C(20)-C(24)	1.418(8)	C(19)-C(20)	1.391(8)
C(21)-C(22)	1.373(8)	C(22)-C(23)	1.399(9)	C(22)-C(25)	1.502(10)
C(23)-C(24)	1.385(8)	C(24)-O(9)	1.363(7)	C(26)-O(9)	1.445(11)
$C(1)_{et}$-$C(2)_{et}$	1.46(2)	$C(2)_{et}$-O_{et}	0.87(2)	C(1)-C(2)-C(3)	113.2(6)
C(1)-C(2)-O(1)	106.5(7)	O(1)-C(2)-C(3)	110.8(7)	C(2)-C(3)-C(4)	116.1(5)
C(2)-C(3)-O(3)	108.6(5)	C(4)-C(3)-O(3)	105.7(5)	C(3)-C(4)-C(5)	104.8(5)
C(3)-C(4)-O(2)	113.5(5)	C(5)-C(4)-O(2)	113.6(4)	C(4)-C(5)-C(6)	103.7(4)
C(4)-C(5)-O(4)	107.8(4)	C(6)-C(5)-O(4)	112.7(4)	C(5)-C(6)-O(3)	103.6(4)
C(5)-C(6)-C(7)	118.8(4)	O(3)-C(6)-C(7)	108.2(4)	C(3)-O(3)-C(6)	107.0(4)
C(6)-C(7)-C(8)	116.4(5)	C(6)-C(7)-C(12)	125.6(5)	C(8)-C(7)-C(12)	118.0(5)
C(7)-C(8)-C(9)	123.0(5)	C(8)-C(9)-C(10)	120.2(5)	C(9)-C(10)-C(11)	121.1(5)
C(10)-C(11)-C(12)	118.0(5)	C(11)-C(12)-C(7)	119.7(5)	C(9)-C(10)-O(5)	116.7(5)
C(11)-C(10)-O(5)	122.2(5)	C(10)-C(11)-C(16)	124.5(5)	C(7)-C(12)-C(13)	125.6(5)
C(11)-C(12)-C(13)	114.7(4)	C(12)-C(13)-C(14)	126.3(5)	C(13)-C(14)-C(15)	116.5(5)
C(14)-C(15)-C(16)	120.1(5)	C(15)-C(16)-C(11)	124.7(5)	C(16)-C(11)-C(12)	117.5(5)
C(11)-C(16)-O(6)	115.1(5)	C(15)-C(16)-O(6)	120.2(5)	C(16)-O(6)-C(17)	117.8(5)
C(12)-C(13)-O(7)	113.4(4)	C(15)-C(14)-C(20)	123.5(5)	O(7)-C(13)-C(14)	120.3(5)
C(13)-O(7)-C(18)	122.9(4)	O(7)-C(18)-C(19)	118.9(4)	C(18)-C(19)-C(20)	119.5(5)
C(19)-C(20)-C(14)	118.1(5)	C(20)-C(14)-C(13)	119.9(5)	C(7)-C(18)-O(8)	117.0(4)
C(19)-C(18)-O(8)	124.1(5)	C(18)-C(19)-C(21)	118.2(5)	C(14)-C(20)-C(24)	126.2(5)
C(20)-C(19)-C(21)	122.3(5)	C(19)-C(21)-C(22)	121.1(5)	C(21)-C(22)-C(23)	117.9(6)
C(21)-C(22)-C(25)	121.6(6)	C(23)-C(22)-C(25)	120.5(6)	C(22)-C(23)-C(24)	121.7(6)
C(23)-C(24)-C(20)	121.3(5)	C(24)-C(20)-C(19)	115.6(5)	C(20)-C(24)-O(9)	117.1(5)
C(23)-C(24)-O(9)	121.6(5)	C(24)-O(9)-C(26)	120.1(6)	$C(1)_{et}$-$C(2)_{et}$-O_{et}	154(2)

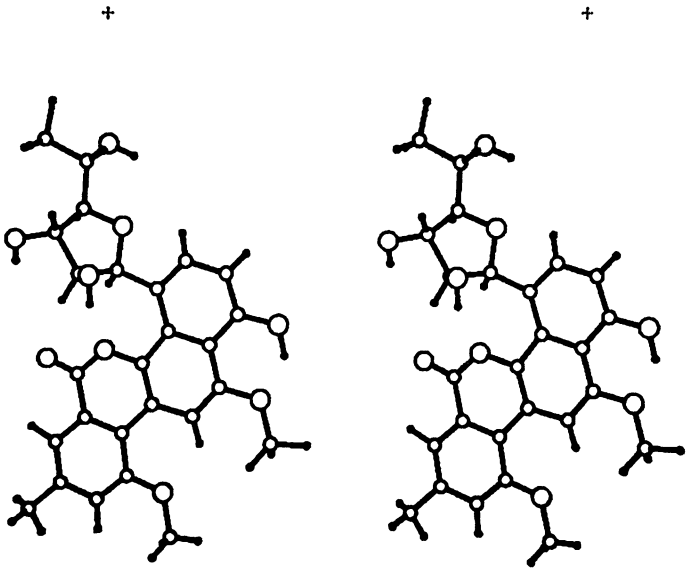

Fig. 2. Stereoscopic drawing of gilvocarcin M.

Table 4. Least-squares planes and dihedral angles (Ψ/°) between them

The asterisked atoms are included in the calculation of the planes and the values in the parentheses are the deviations ($\times 10^3$ Å) from the plane. x, y, and z are in Å

Plane 1. C(3)*[−604], C(4)*[−38], C(5)*[−82], C(6)*[−192], O(3)*[−238]
$0.347x-0.008y-0.938z+0.161=0$

Plane 2. C(3)*[−14], C(4)*[20], C(5)*[−20], C(6)*[13], O(3)[−531]
$0.405x-0.154y-0.901z+0.599=0$

Plane 3. C(7)*[−4], C(8)*[−4], C(9)*[7], C(10)*[−3], C(11)*[−4], C(12)*[8]
$0.211x-0.703y+0.679z+2.653=0$

Plane 4. C(11)*[19], C(12)*[−8], C(13)*[−10], C(14)*[17], C(15)*[−6], C(16)*[−12]
$0.200x-0.683y+0.703z+2.495=0$

Plane 5. O(7)*[25], C(13)*[6], C(14)*[−24], C(18)*[−35], C(19)*[15], C(20)*[13]
$0.161x-0.694y+0.701z+2.816=0$

Plane 6. C(19)*[0], C(20)*[4], C(21)*[−5], C(22)*[6], C(23)*[−2], C(24)*[−3]
$0.124x-0.685y+0.718z+3.045=0$

Plane 7. C(7)*[10], C(8)*[73], C(9)*[107], C(10)*[57], C(11)*[−10], C(12)*[−12], C(13)*[−50], C(14)*[−61], C(15)*[−98], C(16)*[−80], O(7)*[−43], C(18)*[−99], C(19)*[−30], C(20)*[−19], C(21)*[23], C(22)*[100], C(23)*[99], C(24)*[43], C(6)[−42], O(5)[101], O(6)[−92], C(17)[24], O(9)[59], C(26)[109], O(8)[−168]
$0.173x-0.689y+0.704z+2.649=0$

Dihedral angles (Ψ/°)

Plane	2	3	4	5	6	7
1	9.3	56.1	54.2	53.4	51.3	53.5
2		65.3	63.4	62.6	60.6	62.7
3			1.9	3.1	5.5	2.7
4				2.3	4.5	1.6
5					2.4	0.8
6						3.0

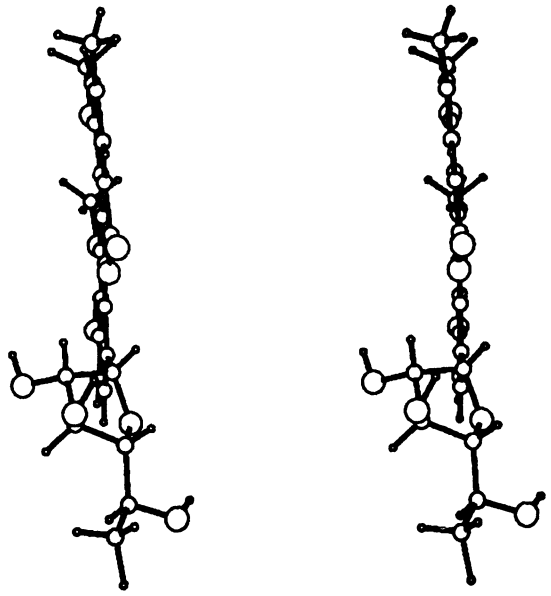

Fig. 3. Stereoscopic side view of gilvocarcin M.

molecules along the c axis, there are two hydrogen bonds; O(2)···O(4) and O(4)···O(8). The third hydrogen bond is formed between the O(1) atom and the oxygen atom of the solvent ethanol. In other part the molecules are stacked mainly by van der Waals interactions. The interplanar separation between the aglycone moieties along the c axis is 3.45 Å.

The solvent molecule of ethanol is disordered, which might be explained by the large cavity around it.

Structure Activity Relationship. It is assumed that the biological activity of gilvocarcins comes mainly from the interaction of the compounds with DNA.[1] It is conceivable from the stereochemical point of view, because gilvocarcins have geometrical prerequisites to interact with DNA. The dimensions and the planarity of the aglycone, and the delocalization of π electrons through the aglycone part are the common structural features found in most antibiotics which interact with DNA through the intercalation mode. It is interesting that gilvocarcins possess partial structures corresponding to K region and bay region[9]

Table 5. Torsional angles (τ/°)

C(1)-C(2)-C(3)-C(4)	−53.5	O(1)-C(2)-C(3)-O(3)	68.0
C(1)-C(2)-C(3)-O(3)	−172.4	O(1)-C(2)-C(3)-C(4)	−173.1
O(3)-C(3)-C(4)-C(5)	−20.1	C(2)-C(3)-C(4)-C(5)	−140.6
O(3)-C(3)-C(4)-O(2)	−144.6	C(2)-C(3)-C(4)-O(2)	94.9
C(3)-C(4)-C(5)-C(6)	−3.3	C(3)-C(4)-C(5)-O(4)	116.4
O(2)-C(4)-C(5)-C(6)	121.1	O(2)-C(4)-C(5)-O(4)	−119.2
C(4)-C(5)-C(6)-O(3)	24.9	C(4)-C(5)-C(6)-C(7)	144.9
O(4)-C(5)-C(6)-O(3)	−91.5	O(4)-C(5)-C(6)-C(7)	28.5
C(5)-C(6)-O(3)-C(3)	−39.4	C(7)-C(6)-O(3)-C(3)	−166.4
C(6)-O(3)-C(3)-C(4)	37.7	C(6)-O(3)-C(3)-C(2)	163.0
C(5)-C(6)-C(7)-C(8)	−97.9	C(5)-C(6)-C(7)-C(12)	83.1
O(3)-C(6)-C(7)-C(8)	19.7	O(3)-C(6)-C(7)-C(12)	−159.3
O(5)-C(10)-C(11)-C(16)	−1.9	C(10)-C(11)-C(16)-O(6)	−0.6
C(15)-C(16)-O(6)-C(17)	−6.7	C(11)-C(16)-O(6)-C(17)	171.5
C(20)-C(24)-O(9)-C(26)	−179.5	C(23)-C(24)-O(9)-C(26)	1.2

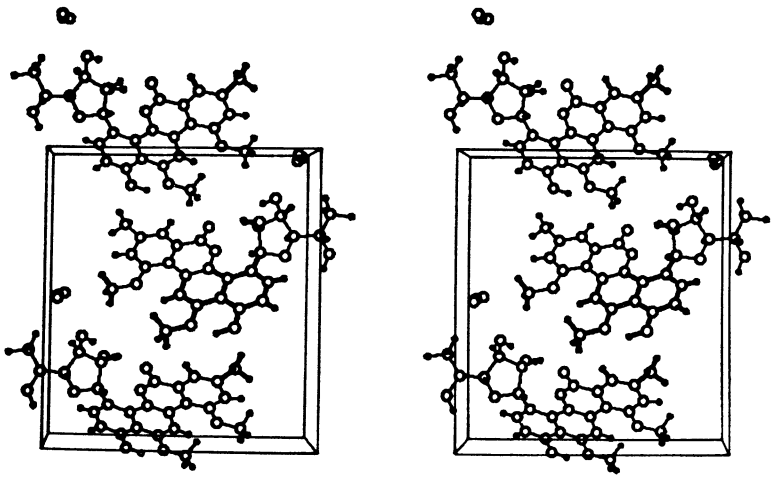

Fig. 4. Crystal structure viewed along c axis.

Table 6. Hydrogen bond distances (l/Å) and angles (ϕ/°)

A-H···B	A···B	∠A-H···B
O(5)-H^{I}···O(6)^{I}	2.547(6)	141(6)
O(1)-H^{I}···O$_{et}^{II}$	2.669(8)	142(6)
O(4)-H^{I}···O(8)^{III}	2.722(5)	168(5)
O(2)-H^{III}···O(4)^{I}	2.770(6)	149(5)
Symmetry code		
I: (x y z)		
II: ($-x$ 0.5+y $-z$)		
III: (x y 1.0+z)		

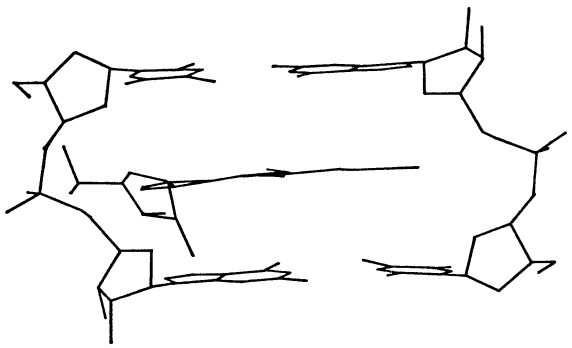

Fig. 5. A hypothetical intercalation mode of gilvocarcin M between the base pairs in DNA.

in the aglycone.

In this connexion, it should be noted that when the methyl group at C(22) is replaced by a vinyl group (gilvocarcin V), the activity is enhanced.[1] The vinyl group is of less bulkiness than the methyl group to intercalate between the base pairs in DNA. In addition to the relief of the steric hindrance, the vinyl group would electronically increase the reactivity of the compound to DNA.

A hypothetical way of the intercalation of gilvocarcin M between the base pairs in DNA is shown in Fig. 5. The structure of the fragment of the unwound DNA is taken from the results of the X-ray analysis of ethidium/dinucleoside monophosphate complex.[10] This figure illustrates that gilvocarcin M has molecular dimensions suitable for intercalation between the base pairs in DNA.

Figures 2, 3, and 4 were drawn by TSD:XTAL, which is a computer-graphics interactive modelling programme for the NOVA3 computer.[11]

References

1) H. Nakano, Y. Matsuda, K. Ito, S. Ohkubo, M. Morimoto, and F. Tomita, *J. Antibiot.*, **34**, 266 (1981).
2) F. Tomita, Y. Matsuda, K. Shirahata, K. Takahashi, H. Nakano, T. Sato, S. Ohkubo, and N. Nakamura, Japan Kokai Koho, 80—57586, April 28 (1980).
3) K. Takahashi, M. Yoshida, F. Tomita, and K. Shirahata, *J. Antibiot.*, **34**, 271 (1981).
4) G. Germain, P. Main, and M. M. Woolfson, *Acta Crystallogr., Sect. A*, **27**, 368 (1971).
5) "International Tables for X-Ray Crystallography," Kynoch Press, Birmingham (1974), Vol. IV, pp. 72—102.
6) A. Pullman and B. Pullman, *Adv Cancer Res.*, **3**, 117 (1955).
7) G. Koyama, H. Nakamura, H. Umezawa, and Y. Iitaka, *Acta Crystallogr., Sect. B*, **32**, 813 (1975).
8) C. Altona and M. Sundaralingam, *J. Am. Chem. Soc.*, **94**, 8205 (1972).
9) D. E. Zacharias, J. P. Glusker, P. P. Fu, and R. G. Harvey, *J. Am. Chem. Soc.*, **101**, 4043 (1979).
10) C. Tsai, S. C. Jain, and H. M. Sobell, *J. Mol. Biol.*, **114**, 301 (1977).
11) A. Takenaka and Y. Sasada, *J. Cryst. Soc. Jpn.*, **22**, 214 (1980).